# 1

# Basics of Polarimetric Scattering

## 1.1 Polarized Electromagnetic Wave

### *1.1.1 Jones Vector and Scattering Matrix*

Radar transmits an electromagnetic (EM) wave and receives the scattered wave from the target. The polarization of an EM wave is defined as the time–space variation of the electric field vector in the plane perpendicular to its propagation direction. As depicted in Figure 1.1, let us first define a coordinate system $(\hat{v}, \hat{h}, \hat{k})$, where $\hat{k}$ denotes the propagation direction, and $\hat{v}, \hat{h}$ denote the directions of vertical and horizontal linear polarizations, respectively. (In this book, unless otherwise specified, vectors are denoted as **bold** letters, for example, **E**, and matrices are **bold** letters with a bar, for example, $\bar{\mathbf{S}}$. A letter with a hat (e.g., $\hat{n}$) denotes a unit vector.) A completely polarized monochromatic EM wave can be represented by two orthogonal components along $\hat{v}, \hat{h}$ (Kong, 2005)

$$\begin{aligned} &\mathbf{E}(z,t) = E_{i0}\hat{e}_i e^{ik_i \cdot r} = \hat{v}E_v + \hat{h}E_h \\ &E_v = E_{0v}\cos(kz - \omega t + \varphi_v), \quad E_h = E_{0h}\cos(kz - \omega t + \varphi_h) \end{aligned} \tag{1.1}$$

where $E_v, E_h$ are the corresponding vertical and horizontal components of the electric field, $k$ is the wavenumber and $\omega$ is the angular frequency. In addition, we have the following relationships, which can be readily derived:

$$\begin{aligned} \mathbf{k} &= k(\hat{x}\sin\theta\cos\phi + \hat{y}\sin\theta\sin\phi + \hat{z}\cos\phi) = k\hat{k} \\ \hat{h} &= \frac{(\hat{z}\times\hat{k})}{|\hat{z}\times\hat{k}|} = -\hat{x}\sin\phi + \hat{y}\cos\phi, \\ \hat{v} &= \hat{h}\times\hat{k} = \hat{x}\cos\theta\cos\phi + \hat{y}\cos\theta\sin\phi - \hat{z}\sin\phi \end{aligned} \tag{1.2}$$

In spherical coordinates, where the source is located at the origin, we have $\hat{v} = \hat{\theta}$, $\hat{h} = \hat{\phi}$, $\hat{k} = \hat{r}$.

Imagine when an EM wave passes a certain position in space; the tip of the electric field vector will form a certain trajectory. The shape of such a trajectory is determined by the

*Polarimetric Scattering and SAR Information Retrieval*, First Edition. Ya-Qiu Jin and Feng Xu.
© 2013 John Wiley & Sons Singapore Pte. Ltd. Published 2013 by John Wiley & Sons Singapore Pte. Ltd.

COPYRIGHTED MATERIAL

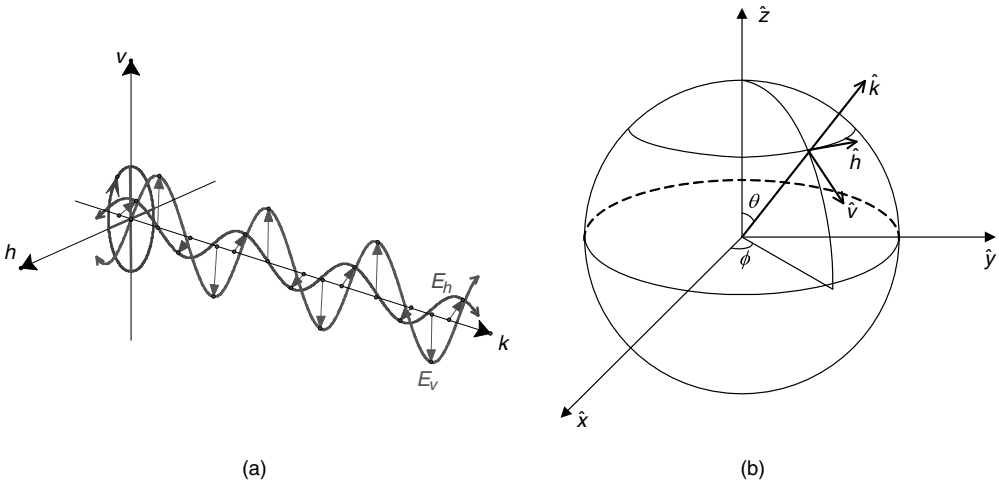



**Figure 1.1** (a) Polarized EM wave and polarization vector. (b) Coordinate system of the polarization vector

amplitude ratio and phase difference between the two orthogonal components, that is, the polarization ratio,

$$|\rho| = E_{0h}/E_{0v}, \quad \varphi = \varphi_h - \varphi_v \tag{1.3}$$

The polarization of an EM wave is named after the shape of such a trajectory, that is, linear polarization (when $\varphi = m\pi$, $m = 0, 1, 2, \ldots$), circular polarization (when $\varphi = m\pi + \pi/2$, $m = 0, 1, 2, \ldots$, and $E_{0v} = E_{0h}$) or elliptical polarization (in general). The trajectories of

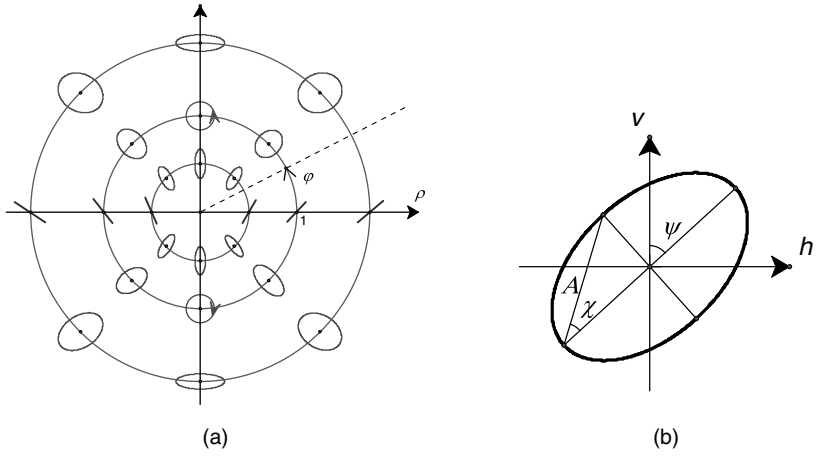



**Figure 1.2** (a) Plane of polarization ratio. (b) Parameters of elliptical polarization

different polarizations are depicted accordingly in the $(|\rho|, \varphi)$ plane as in Figure 1.2a. In fact, any polarization trajectory can be expressed using the following ellipse equation:

$$\left(\frac{E_v}{E_{0v}}\right)^2 - 2\frac{E_v E_h}{E_{0v}E_{0h}}\cos\varphi + \left(\frac{E_h}{E_{0h}}\right)^2 = \sin\varphi \tag{1.4}$$

There are three geometric parameters of such an elliptical trajectory: amplitude $A$, elliptical angle $\chi$, and orientation $\psi$, as illustrated in Figure 1.2b, that is

$$\begin{aligned} &A = \sqrt{E_{0v}^2 + E_{0h}^2}, \\ &|\sin 2\chi| = 2\frac{E_{0v}E_{0h}}{E_{0v}^2 + E_{0h}^2}|\sin\varphi|, \quad \tan 2\psi = 2\frac{E_{0v}E_{0h}}{E_{0v}^2 - E_{0h}^2}\cos\varphi \end{aligned} \tag{1.5}$$

where the sign of $\chi$ indicates the rotation direction, that is, counter-clockwise $(+)$ or clockwise $(-)$, the elliptical angle $\chi$ determines the shape, and $\psi$ indicates orientation.

We can write Equation 1.1 in the form of a complex vector,

$$\mathbf{E} = \begin{bmatrix} E_v \\ E_h \end{bmatrix} = \begin{bmatrix} E_{0v}e^{i\varphi_v} \\ E_{0h}e^{i\varphi_h} \end{bmatrix} \tag{1.6}$$

which is often referred to as the Jones vector. It can be found from Equation 1.3 that the polarization ratio is in fact the ratio of these two elements

$$\rho = |\rho|e^{i\varphi} = \frac{E_{0h}e^{i\varphi_h}}{E_{0v}e^{i\varphi_v}} \tag{1.7}$$

The Jones vector can also be expressed using the elliptical parameters,

$$\mathbf{E} = Ae^{i\varphi_0}\begin{bmatrix} \cos\psi & -\sin\psi \\ -\sin\psi & \cos\psi \end{bmatrix}\begin{bmatrix} \cos\chi \\ i\sin\chi \end{bmatrix} \tag{1.8}$$

where $\varphi_0$ is the absolute phase. It can be seen from Equation 1.8 that transformation of the Jones vector would correspondingly modify polarization characteristics. This is important in radar polarimetry, as will be discussed later in Chapter 5.

A completely polarized wave incident upon a point target or deterministic simple target would produce a completely polarized scattered wave, which is often called coherent scattering. As a polarized wave $\mathbf{E}_i = \hat{e}_i E_{i0} e^{i\mathbf{k}_i\cdot\mathbf{r}}$ incident on a scatterer of volume $v_0$ and dielectric constant $\varepsilon_{sn}$ $(= \varepsilon_s/\varepsilon_0)$, the wave equation can be written as (Jin, 1994)

$$\nabla\times\nabla\times\mathbf{E}(\mathbf{r}) + k^2\mathbf{E}(\mathbf{r}) = \begin{cases} -i\omega\varepsilon_0(\varepsilon_{sn}-1), & \mathbf{r}\in v_0 \\ 0, & \mathbf{r}\notin v_0 \end{cases} \tag{1.9}$$

where the time-harmonic factor is $e^{-i\omega t}$ $(i = -j = \sqrt{-1})$ and $r$ is the distance from the scattering point to the observation point. Solving Equation 1.9 under the far-field approximation

yields the scattering $\mathbf{E}_s$wave

$$\begin{aligned}\mathbf{E}_s(r) &= -\frac{e^{ikr}}{r}k^2\int_{v_0}\hat{k}_s\times[\hat{k}_s\times\mathbf{E}(\mathbf{r}')][\varepsilon_{sn}(\mathbf{r}')-1]e^{-i\mathbf{k}_s\cdot\mathbf{r}'}d\mathbf{r}' \\ &= \frac{e^{ikr}}{r}k^2\int_{v_0}(\hat{v}_s\hat{v}_s+\hat{h}_s\hat{h}_s)[\varepsilon_{sn}(\mathbf{r}')-1]\mathbf{E}(\mathbf{r}')e^{-i\mathbf{k}_s\cdot\mathbf{r}'}d\mathbf{r}' \\ &\equiv \frac{e^{ikr}}{r}\overline{\mathbf{S}}\cdot\mathbf{E}_i = \frac{e^{ikr}}{r}\begin{bmatrix}S_{vv} & S_{vh}\\ S_{hv} & S_{hh}\end{bmatrix}\cdot\mathbf{E}_i\end{aligned} \tag{1.10}$$

Here, the scattering field is now expressed by a $2\times 2$ (dimensional) complex matrix, that is, the scattering matrix, $\bar{\mathbf{S}}$. Each element of the scattering matrix $S_{pq}$, $p,q=v,h$, represents the complex scattering coefficient under $q$-polarization incidence and $p$-polarization scattering.

For a single scattering, its scattering matrix has to be obtained by first calculating the internal field $\mathbf{E}(\mathbf{r}')$ in Equation 1.10 and then performing the integration. Explicit solutions exist for many canonical problems. For example, a small scatterer with its size $a$ far smaller than the wavelength, that is, $ka\ll 1$, can be solved by Rayleigh approximation. A non-spherical particle such as an ellipsoid, a needle- or a disk-like particle with its smallest dimension $d$ far smaller than the wavelength, that is, $kd(\varepsilon_{sn}-1)\ll 1$, can be solved using the Rayleigh–Gans approximation (Ishimaru, 1978, 1991). A scatterer of perfectly spherical geometry can be solved using Mie theory. Explicit expressions for $\bar{\mathbf{S}}$ also exist for symmetric geometries such as cylinders, spheroids, and so on. Analytic calculations of the scattering matrix for these examples under the Rayleigh–Gans approximation are given later in this chapter. For a more complete derivation, readers are referred to the literature focusing on EM theory (e.g., Jin, 1994).

For a large scattering body with complicated geometry, we have to resort to numerical methods such as the method of momentss (MoM), finite element method (FEM), and finite difference time difference (FDTD), or high-frequency methods such as geometrical optics and physical optics. Chapter 11 will introduce a high-frequency method for calculation of scattering from very complex targets in natural environments.

In practice, fully polarimetric radar measures the entire scattering matrix $\bar{\mathbf{S}}$, while single-polarization radar (single-pol) or dual-polarization radar (dual-pol) can only measure one or two elements of the scattering matrix. Conventionally, co-pol refers to scattering with the same polarization for incidence and scattering, while cross-pol refers to different polarization for incidence and scattering.

Another important concept is the scattering coefficient or radar cross-section (RCS). It is defined as the power ratio of scattering versus incidence as if the scattered field were uniform in all directions:

$$\sigma_{pq} = 4\pi\left|S_{pq}\right|^2 \quad (\mathrm{m}^2) \tag{1.11}$$

The RCS is more useful for single-polarization radar where phase information is not critical.

### *1.1.2 Stokes Vector and Mueller Matrix*

As opposed to coherent scattering for a single deterministic target, incoherent scattering is from random or distributed targets, for example, random discrete particles, random media,

and randomly rough surfaces. Incoherent scattering is studied from a statistical perspective. That is based on the second-order moment of the random field $\langle \mathbf{E}_s \mathbf{E}_s^* \rangle$, which is in the unit of power.

Incoherent scattering produces a partially polarized wave, which is usually described using the Stokes vector $\mathbf{I}$, which consists of four Stokes parameters as follows:

$$\begin{aligned} I &= \frac{1}{\eta}\left\langle |E_v|^2 + |E_h|^2 \right\rangle = \frac{1}{\eta}\left\langle E_{0v}^2 + E_{0h}^2 \right\rangle \\ Q &= \frac{1}{\eta}\left\langle |E_v|^2 - |E_h|^2 \right\rangle = \frac{1}{\eta}\left\langle E_{0v}^2 - E_{0h}^2 \right\rangle \\ U &= \frac{1}{\eta} 2\,\mathrm{Re}\left\langle E_v E_h^* \right\rangle = \frac{1}{\eta} 2\langle E_{0v} E_{0h} \cos\varphi \rangle \\ V &= \frac{1}{\eta} 2\,\mathrm{Im}\left\langle E_v E_h^* \right\rangle = \frac{1}{\eta} 2\langle E_{0v} E_{0h} \sin\varphi \rangle \end{aligned} \tag{1.12}$$

where $*$ denotes conjugate, $\eta$ denotes wave impedance, and $\langle \cdot \rangle$ denotes the ensemble average. Stokes law gives

$$I^2 \geq Q^2 + U^2 + V^2 \tag{1.13}$$

where the equality only holds for a completely polarized wave. For a completely polarized wave, only three of the Stokes parameters in Equation 1.12 are independent. This corresponds to the above-mentioned three geometric parameters of elliptical polarization:

$$\mathbf{I} = \begin{bmatrix} I \\ I\cos 2\psi \cos 2\chi \\ I \sin 2\psi \cos 2\chi \\ I \sin 2\chi \end{bmatrix} \tag{1.14}$$

With given intensity $I$, any complete polarization can be mapped into a point on a sphere in 3D $(Q, U, V)$ space. The sphere with radius $I$ is referred to as the Poincaré sphere. Partial polarizations will be distributed inside the Poincaré sphere. Interestingly, two angles defining a 3D vector pointing to any point on the Poincaré sphere are equal to the parameters $2\chi, 2\psi$ of the elliptical polarization on that point. Thus, we can draw the distribution of polarizations on the Poincaré sphere as in Figure 1.3. It can be directly mapped to the polarization ratio plane in Figure 1.2.

Another commonly used form of Stokes parameters are defined as

$$I_v = \frac{1}{\eta}\left\langle |E_v|^2 \right\rangle, \quad I_h = \frac{1}{\eta}\left\langle |E_h|^2 \right\rangle, \quad U = \frac{1}{\eta} 2\,\mathrm{Re}\left\langle E_v E_h^* \right\rangle, \quad V = \frac{1}{\eta} 2\,\mathrm{Im}\left\langle E_v E_h^* \right\rangle \tag{1.15}$$

These two definitions of Stokes parameters can be transformed into one another.

Incoherent scattering of random or distributed targets has a depolarization effect, which renders the scattered wave to be a partially polarized wave. Using Stokes vectors $\mathbf{I}_i$, $\mathbf{I}_s$ to

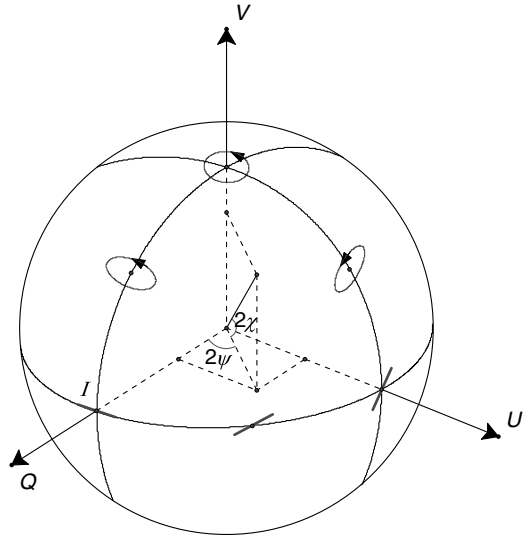



**Figure 1.3** Poincaré sphere

represent the incident and scattered wave, respectively, the incoherent scattering is then represented using a $4 \times 4$ real Mueller matrix

$$\mathbf{I}_s = \overline{\mathbf{M}} \cdot \mathbf{I}_i \tag{1.16}$$

The Mueller matrix is in fact the second-order moment of the scattering matrix. From Equations 1.10 and 1.15, we have

$$\overline{\mathbf{M}} = \begin{bmatrix} \left\langle |S_{vv}|^2 \right\rangle & \left\langle |S_{vh}|^2 \right\rangle & \mathrm{Re}\left\langle S_{vv}S_{vh}^* \right\rangle & -\mathrm{Im}\left\langle S_{vv}S_{vh}^* \right\rangle \\ \left\langle |S_{hv}|^2 \right\rangle & \left\langle |S_{vv}|^2 \right\rangle & \mathrm{Re}\left\langle S_{hv}S_{hh}^* \right\rangle & -\mathrm{Im}\left\langle S_{hv}S_{vh}^* \right\rangle \\ 2\,\mathrm{Re}\left\langle S_{vv}S_{hv}^* \right\rangle & 2\,\mathrm{Re}\left\langle S_{vh}S_{hh}^* \right\rangle & \mathrm{Re}\left\langle S_{vv}S_{hh}^* + S_{vh}S_{hv}^* \right\rangle & -\mathrm{Im}\left\langle S_{vv}S_{hh}^* - S_{vh}S_{hv}^* \right\rangle \\ 2\,\mathrm{Im}\left\langle S_{vv}S_{hv}^* \right\rangle & 2\,\mathrm{Im}\left\langle S_{vh}S_{hh}^* \right\rangle & \mathrm{Im}\left\langle S_{vv}S_{hh}^* + S_{vh}S_{hv}^* \right\rangle & \mathrm{Re}\left\langle S_{vv}S_{hh}^* - S_{vh}S_{hv}^* \right\rangle \end{bmatrix} \tag{1.17}$$

Some useful conclusions about the Mueller matrix are given here. For coherent scattering, only seven of the 16 elements of the Mueller matrix are independent, which corresponds to seven degrees of freedom in the scattering matrix (the ensemble average eliminates the absolute phase). For most natural targets, co-polarization and cross-polarization are not correlated, which makes the eight elements in the top-right and bottom-left quarters approach zero. For the remaining eight elements, the top-left quartet reflect the average power of the two polarizations and the bottom-right quartet reflect the correlation between different polarizations.

From the Mueller matrix, we can also derive polarization signatures of the target, which are defined as follows:

co-polarization signature

$$\sigma_c(\chi, \psi) = 4\pi \cdot \frac{1}{2}\mathbf{I}_s^{\mathrm{T}} \cdot \mathbf{I}_i(\chi, \psi) \tag{1.18}$$

cross-polarization signature

$$\sigma_x(\chi,\psi) = 4\pi \cdot \frac{1}{2}\left[\mathbf{I}_s^{\mathrm{T}} \cdot \mathbf{I}_s - \mathbf{I}_s^{\mathrm{T}} \cdot \mathbf{I}_i(\chi,\psi)\right] \tag{1.19}$$

where the superscript T denotes transpose. Note that polarization signatures $\sigma_c(\chi,\psi)$, $\sigma_d(\chi,\psi)$ are in fact the co-polarized (co-pol) and cross-polarized (cross-pol) scattering coefficients under elliptical polarization incidence of the parameters $\chi,\psi$. Substituting $\chi = 0^\circ, \psi = 0^\circ$ or $\chi = 0^\circ, \psi = 90^\circ$ into Equation 1.19, it gives the horizontally or vertically co-pol and cross-pol scattering coefficients.

In addition, we have the polarization degree defined as

$$m_s = \frac{Q_s^2 + U_s^2 + V_s^2}{I_s^2} \tag{1.20}$$

and the co-pol/cross-pol phase difference as

$$\phi_{vh} = \tan^{-1}\frac{M_{43} - M_{34}}{M_{33} + M_{44}} \tag{1.21}$$

and $M_{ij}$ denotes the $i,j$ element of the Mueller matrix $\overline{\mathbf{M}}$. Clearly, we have the inequality $m_s \leq 1$, where $m_s = 1$ when the scattered Stokes intensity $\mathbf{I}_s$ is completely polarized. The quantity $[Q_s^2 + U_s^2 + V_s^2]^{1/2}$ denotes a point inside the Poincaré sphere, and the radius of the Poincaré sphere is equal to $I$.

Table 1.1 gives few examples of the scattering matrix of ideal scattering targets. The corresponding polarization signatures are given in Figure 1.4.

**Table 1.1** Example scattering matrices of ideal scattering targets

| | |
|---|---|
| Sphere, Plane, or Corner reflector | $S = \begin{bmatrix} 1 & 0 \\ 0 & -1 \end{bmatrix}$ |
| Diplane | $S = \begin{bmatrix} 1 & 0 \\ 0 & 1 \end{bmatrix}$ |
| Diplane (45° tilted) | $S = \begin{bmatrix} 0 & 1 \\ -1 & 0 \end{bmatrix}$ |
| Dipole (vertically oriented) | $S = \begin{bmatrix} 1 & 0 \\ 0 & 0 \end{bmatrix}$ |
| Dipole (45° tilted) | $S = \begin{bmatrix} 1 & 1 \\ -1 & -1 \end{bmatrix}$ |
| Helix (right-handed) | $S = \begin{bmatrix} 1 & i \\ -i & 1 \end{bmatrix}$ |
| Helix (left-handed) | $S = \begin{bmatrix} 1 & -i \\ i & 1 \end{bmatrix}$ |

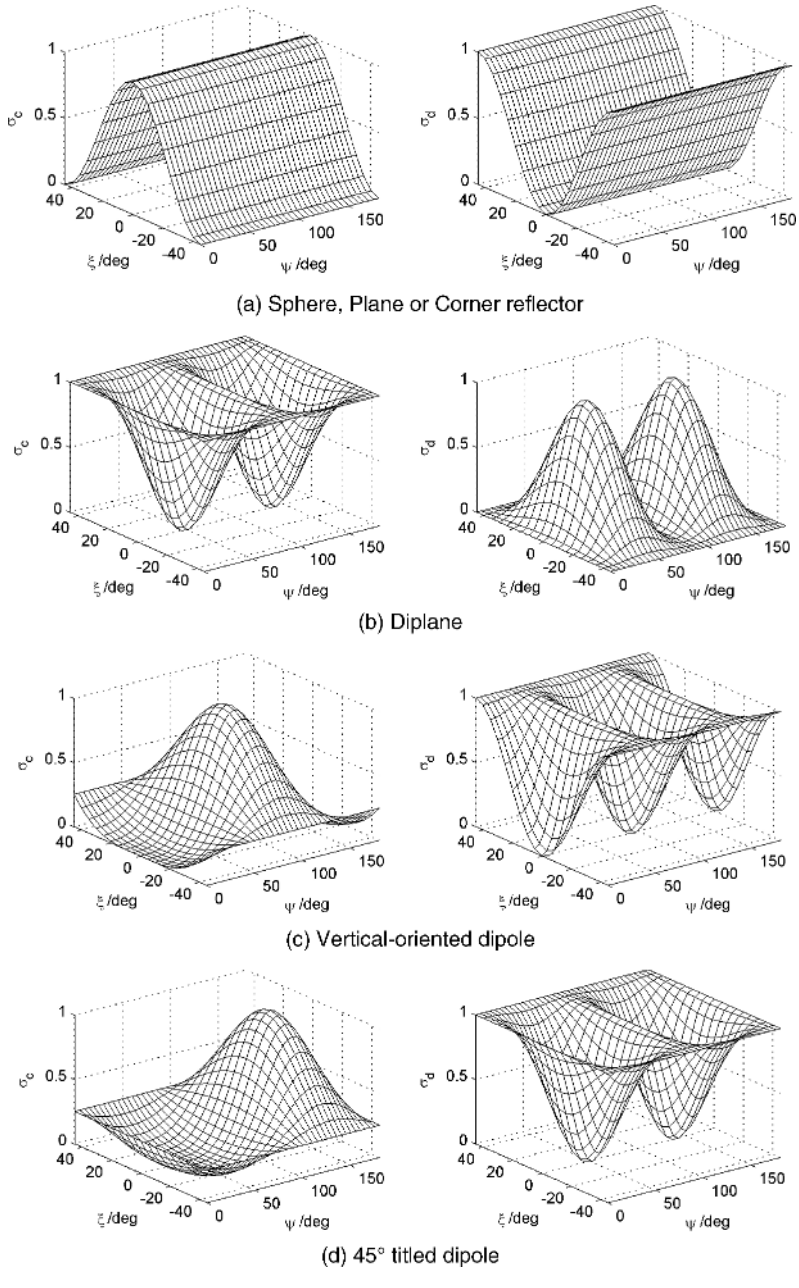
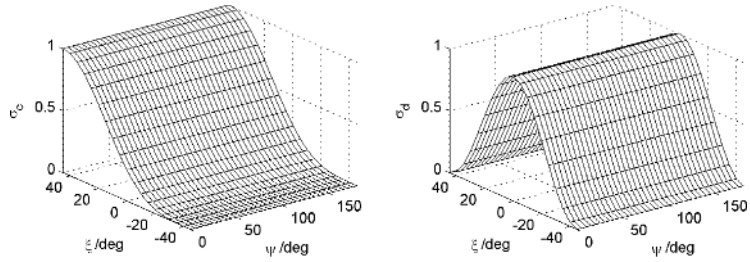



**Figure 1.4** Co-pol and cross-pol signatures of ideal targets




(e) Right-hand helix

**Figure 1.4** (*Continued*)

## 1.2 Volumetric Scattering

### *1.2.1 Small Particle under Rayleigh–Gans Approximation*

Small-particle scattering is common in natural environments, and thus is very useful for remote sensing studies. For modeling scattering of the vegetation canopy, we mainly use the Rayleigh–Gans approximation of non-spherical particles including spheroids, disk-like and needle-like particles (Ishimaru, 1978; Jin, 1994).

Under the Rayleigh approximation, the term in Equation 1.10 becomes $\exp(-i\mathbf{k}_s \cdot \mathbf{r}') \approx 1$, that is, it ignores the coherent effect of different elements inside the particle. The internal field $\mathbf{E}(\mathbf{r}')$ can be obtained using electrostatic principles. Hence, the scattering matrix can be calculated.

For non-spherical particles whose smallest dimension meets the condition $kd(\varepsilon_{sn} - 1) \ll 1$, we can still use the Rayleigh–Gans approximation, where the internal field is approximated as $\mathbf{E}(\mathbf{r}') \approx \hat{e}_i E_0 \exp(i\mathbf{k}_i \cdot \mathbf{r}')$. However, the term $\exp[i(\mathbf{k}_i - \mathbf{k}_s) \cdot \mathbf{r}']$ is kept in order to account for the coherent effect of different elements, that is

$$\mathbf{E}_s(r) = \frac{e^{ikr}}{r}\frac{k^2}{4\pi}(\hat{v}_s\hat{v}_s + \hat{h}_s\hat{h}_s) \cdot \bar{\mathbf{A}}_b \cdot \hat{e}_i E_0 \int_{v_0} [\varepsilon_{sn}(\mathbf{r}') - 1] e^{i(\mathbf{k}_i - \mathbf{k}_s)\cdot\mathbf{r}'} d\mathbf{r}' \tag{1.22}$$

Notice that the above integral is in fact the Fourier transform of $\varepsilon_{sn} - 1$ in the direction $\mathbf{k}_i - \mathbf{k}_s$. If $\varepsilon_{sn} - 1$ is limited to within a small region, the scattering is smooth along the wavenumber domain $\mathbf{k}_i - \mathbf{k}_s$, that is, it is a smooth angular distribution, which is close to Rayleigh scattering. On the other hand, the scattering will focus on a narrow forward direction, with a complicated angular distribution. In this sense, it resembles the relationship between time-domain and frequency-domain signals.

Given a small ellipsoid of semi-axes $a, b, c$ and volume $v_0 = (4\pi/3)abc$, the term $\bar{\mathbf{A}}_b$ in Equation 1.22 can be obtained as

$$\overline{\mathbf{A}}_b = \sum_{n=1}^{3} \frac{\hat{x}_n\hat{x}_n}{1 + (\varepsilon_s/\varepsilon_0 - 1)g_n}, \quad \hat{x}_1 = \hat{x}_b,\ \hat{x}_2 = \hat{y}_b,\ \hat{x}_3 = \hat{z}_b \tag{1.23}$$

where $\hat{x}_b, \hat{y}_b, \hat{z}_b$ denotes the local coordinates of the ellipsoid, $g_1$ is expressed as

$$g_1 = \frac{abc}{2}\int_0^\infty ds \frac{1}{(s+a^2)R_s}, \quad R_s = [(s+a^2)(s+b^2)(s+c^2)]^{1/2} \tag{1.24}$$

and $g_2, g_3$ can be expressed in the same way as $g_1$ with $a$ replaced by $b, c$, respectively. It can be found that $g_1 + g_2 + g_3 = 1$.

The scattering matrix is thus derived as

$$\begin{aligned} &S_{pq}(\theta,\phi;\theta',\phi') = \hat{p}\cdot\overline{\mathbf{T}}\cdot\hat{q}', \qquad p,q = v,h \\ &\overline{\mathbf{T}} = \sum_{n=1}^{3} T_n \hat{x}_n \hat{x}_n, \quad T_n = \frac{3}{2k} t_n (1+it_n), \quad t_n = \frac{2}{9}k^3 abc \frac{\varepsilon_s/\varepsilon_0 - 1}{1+(\varepsilon_s/\varepsilon_0 - 1)g_n} \end{aligned} \tag{1.25}$$

Note that the imaginary part of $T_n$ is included so that the scattering matrix $S_{pq}$ can be accurate enough when later used to calculate the extinction coefficient under the optics theorem in Chapter 2.

Assuming that the ellipsoid is rotationally symmetric, that is, $a = b$, which is the case for most particles in the natural environment, then the scattering matrix can be expanded to

$$\begin{aligned} S_{vv}(\theta_s,\phi_s;\theta_i,\phi_i) &= \frac{3}{2k}\left[T_1(\hat{\theta}_s\cdot\hat{\theta}_i) + (T_0 - T_1)(\hat{\theta}_s\cdot\hat{z}_b)(\hat{z}_b\cdot\hat{\theta}_i)\right] \\ S_{vh}(\theta_s,\phi_s;\theta_i,\phi_i) &= \frac{3}{2k}\left[T_1(\hat{\theta}_s\cdot\hat{\phi}_i) + (T_0 - T_1)(\hat{\theta}_s\cdot\hat{z}_b)(\hat{z}_b\cdot\hat{\phi}_i)\right] \\ S_{hv}(\theta_s,\phi_s;\theta_i,\phi_i) &= \frac{3}{2k}\left[T_1(\hat{\phi}_s\cdot\hat{\theta}_i) + (T_0 - T_1)(\hat{\phi}_s\cdot\hat{z}_b)(\hat{z}_b\cdot\hat{\theta}_i)\right] \\ S_{hh}(\theta_s,\phi_s;\theta_i,\phi_i) &= \frac{3}{2k}\left[T_1(\hat{\phi}_s\cdot\hat{\phi}_i) + (T_0 - T_1)(\hat{\phi}_s\cdot\hat{z}_b)(\hat{z}_b\cdot\hat{\phi}_i)\right] \end{aligned} \tag{1.26}$$

Note that the orientation of the particle's symmetry axis is represented by $\hat{z}_b$.

Calculating the integral of Equation 1.24, we have

$$\begin{aligned} g_1 &= \frac{1}{2}(1-g_3) \\ g_3 &= \begin{cases} \dfrac{a^2}{a^2-c^2}\left[1 - \dfrac{c}{\sqrt{a^2-c^2}}\tan^{-1}\dfrac{\sqrt{a^2-c^2}}{c}\right] & \text{if } a = b > c \\ \dfrac{a^2}{a^2-c^2}\left[1 + \dfrac{c}{2\sqrt{c^2-a^2}}\ln\dfrac{c-\sqrt{c^2-a^2}}{c+\sqrt{c^2-a^2}}\right] & \text{if } a = b < c \end{cases} \end{aligned} \tag{1.27}$$

where the two cases correspond to prolate and oblate ellipsoids, respectively.

For a disk-like particle, with radius $a$, height $2h$, and volume $v_0 = 2\pi a^2 h$, and given $h \ll a$, the integral of Equation 1.22 can be derived as

$$\int_{v_0} d\mathbf{r}' \exp[-i(\mathbf{k}_i - \mathbf{k}_s) \cdot \mathbf{r}'] = \frac{2J_1\left[ka\sqrt{\sin^2\theta_s + \sin^2\theta_i - 2\sin\theta_s \sin\theta_i \cos(\phi_s - \phi_i)}\right]}{ka\sqrt{\sin^2\theta_s + \sin^2\theta_i - 2\sin\theta_s \sin\theta_i \cos(\phi_s - \phi_i)}} \quad (1.28)$$

$$g_3 = \frac{(a/h)^2}{(a/h)^2 - 1}\left[1 - \frac{1}{\sqrt{(a/h)^2 - 1}} \sin^{-1}\left(\frac{\sqrt{(a/h)^2 - 1}}{a/h}\right)\right] \quad (1.29)$$

where $J_1(\cdot)$ denotes the first-order Bessel function of the first kind.

For a needle-like particle with radius $a$, length $2h$, and volume $v_0 = 2\pi a^2 h$, and given $h \gg a$, the integral in Equation 1.22 can be derived as

$$\int_{v_0} d\mathbf{r}' \exp[-i(\mathbf{k}_i - \mathbf{k}_s) \cdot \mathbf{r}'] = \frac{\sin[kh(\cos\theta_i + \cos\theta_s)]}{kh(\cos\theta_i + \cos\theta_s)} \quad (1.30)$$

$$g_3 = -\frac{(a/h)^2}{1 - (a/h)^2}\left[1 + \frac{1}{2\sqrt{1 - (a/h)^2}} \log\left(\frac{1 - \sqrt{1 - (a/h)^2}}{1 + \sqrt{1 - (a/h)^2}}\right)\right] \quad (1.31)$$

Under extreme conditions, $h \ll a$ and $h \gg a$, Equations 1.29 and 1.31 are consistent with Equation 1.27.

These expressions are critical in computing the scattering matrix, phase matrix, and extinction coefficient, and for modeling the scattering behavior of random particles in the vegetation canopy.

### *1.2.2 Slim Cylinder*

A finite-length slim cylinder is often used to model the trunk, branches or twigs of trees. Its scattering can be solved as in Equation 1.10

$$\mathbf{E}_s(\mathbf{r}) = \frac{e^{ikr}}{r} k^2 \int_{v_0} (\hat{v}_s \hat{v}_s + \hat{h}_s \hat{h}_s)[\varepsilon_{sn}(\mathbf{r}') - 1]\mathbf{E}(\mathbf{r}') e^{-i\mathbf{k}_s \cdot \mathbf{r}'} d\mathbf{r}' \quad (1.32)$$

where the internal field term $\mathbf{E}(\mathbf{r}')$ can be approximated as if it was an infinitely long cylinder, for which the explicit solution can be found. The internal field of an infinitely long cylinder can be found, for example, in Wait (1986) and Karam and Fung (1988). Substituting $\mathbf{E}(\mathbf{r}')$ into Equation 1.32 and completing the integral, it yields the explicit expression of the scattering field $\mathbf{E}_s$ and hence the scattering matrix $\overline{\mathbf{S}}$ (Karam and Fung, 1988).

Given the cylinder parameters of length $2L$ and radius $a$, the dielectric constant $\varepsilon_{sn}$ $(= \varepsilon_s/\varepsilon_0)$, and the fact that its axis is aligned with $\hat{z}$, the scattering matrix $\overline{\mathbf{S}}$ for a cylinder can be derived as

$$S_{vv}(\theta_s,\theta_i,\phi_s-\phi_i)=k_0^2L(\varepsilon_{sn}-1)\mu_{si}\{(e_{n0}B_0\cos\theta_s\cos\theta_i-Z_0\sin\theta_s)+2\sum_{n=1}^{\infty}[(e_{nv}B_n\cos\theta_i+i\eta h_{nv}A_n)\cos\theta_s-e_{nv}Z_n\sin\theta_s]\cos[n(\phi_s-\phi_i)]\} \tag{1.33}$$

$$S_{hh}(\theta_s,\theta_i,\phi_s-\phi_i)=k_0^2L(\varepsilon_{sn}-1)\mu_{si}\left\{B_0\eta h_{0h}+2\sum_{n=1}^{\infty}[(\eta h_{nh}B_n-ie_{nh}A_n\cos\theta_i)\cos[n(\phi_s-\phi_i)]\right\} \tag{1.34}$$

$$S_{vh}(\theta_s,\theta_i,\phi_s-\phi_i)=-2ik_0^2L(\varepsilon_{sn}-1)\mu_{si}\sum_{n=1}^{\infty}[(e_{nh}B_n\cos\theta_i+i\eta h_{nh}A_n)\cos\theta_s-e_{nh}Z_n\sin\theta_s]\sin[n(\phi_s-\phi_i)]\} \tag{1.35}$$

$$S_{hv}(\theta_s,\theta_i,\phi_s-\phi_i)=-2ik_0^2L(\varepsilon_{sn}-1)\mu_{si}\sum_{n=1}^{\infty}[(\eta h_{nv}B_n-ie_{nv}A_n\cos\theta_i)\sin[n(\phi_s-\phi_i)]\} \tag{1.36}$$

where

$$\begin{aligned}A_n&=\frac{k_0}{2k_{1\rho}}(Z_{n-1}-Z_{n+1}),\quad B_n=\frac{k_0}{2k_{1\rho}}(Z_{n-1}+Z_{n+1})\\ Z_n&=\frac{a^2}{u^2-v_s^2}[uJ_n(v_s)J_{n+1}(u)-v_sJ_n(u)J_{n+1}(v_s)]\end{aligned} \tag{1.37}$$

$$\begin{aligned}u=k_{1\rho}a,\quad v_s=k_0a\sin\theta_s,\quad v_i=k_0a\sin\theta_i,\quad k_{1\rho}=k_0\sqrt{(\varepsilon_{sn}-\cos^2\theta_i)}\\ \mu_{si}=\frac{\sin[k_0L(\cos\theta_i+\cos\theta_s)]}{k_0L(\cos\theta_i+\cos\theta_s)},\quad \eta=\sqrt{\frac{\mu_0}{\varepsilon_0}}\end{aligned} \tag{1.38}$$

$$e_{nv}=-\frac{i\sin\theta_i}{R_nJ_n(u)}\left[\frac{H_n^{(2)'}(v_i)}{v_iH_n^{(2)}(v_i)}-\frac{J_n'(u)}{uJ_n(u)}\right],\quad e_{nh}=-\frac{\sin\theta_i}{R_nJ_n(u)}\left[\frac{1}{v_i^2}-\frac{1}{u^2}\right] \tag{1.39}$$

$$\eta h_{nv}=\frac{\sin\theta_i}{R_nJ_n(u)}\left[\frac{1}{v_i^2}-\frac{1}{u^2}\right]n\cos\theta_i,\quad \eta h_{nh}=-\frac{\sin\theta_i}{R_nJ_n(u)}\left[\frac{H_n^{(2)'}(v_i)}{v_iH_n^{(2)}(v_i)}-\frac{\varepsilon_{sn}J_n'(u)}{uJ_n(u)}\right] \tag{1.40}$$

and

$$R_n=\frac{1}{2}\pi v_i^2H_n^{(2)}(v_i)\left\{\left[\frac{H_n^{(2)'}(v_i)}{v_iH_n^{(2)}(v_i)}-\frac{J_n'(u)}{uJ_n(u)}\right]\times\left[\frac{H_n^{(2)'}(v_i)}{v_iH_n^{(2)}(v_i)}-\frac{\varepsilon_{sn}J_n'(u)}{uJ_n(u)}\right]-\left(\frac{1}{u^2}-\frac{1}{v_i^2}\right)^2n^2\cos^2\theta_i\right\} \tag{1.41}$$

Note that $J_n(u)$ and $J_n'(u)$ stand for the $n$th-order Bessel function and its derivative, respectively; and $H_n^{(2)}(v_i)$ and $H_n^{(2)'}(v_i)$ are the $n$th-order Hankel function of the second kind and its derivative, respectively.

It can be seen from Equations 1.35 and 1.36 that there is no cross-polarized backscattering, that is, $S_{vh} = S_{hv} = 0$ under the condition $\phi_s = \pi + \phi_i$.

Interestingly, it can be found that, if $k_0 L \gg 1$ and $\cos\theta_i + \cos\theta_s \neq 0$, then $\mu_{si} = 0$ in Equation 1.38; if $\cos\theta_i + \cos\theta_s = 0$, then $\mu_{si} = 1$, which means that the scattered wave propagates along the cone surface forming angle $\theta_i$ with respect to axis $\hat{z}$.

In the general case when the cylinder orientation $\hat{z}_\ell$ differs from the global coordinate $\hat{z}$, then the above expressions should be defined in its local coordinates $(\hat{x}_\ell, \hat{y}_\ell, \hat{z}_\ell)$. The scattering field in Equation 1.32 and the scattering matrix in Equations 1.33–1.36 have to be further converted to the global coordinate system via coordinate conversions, which will be introduced in subsection 1.3.7.

## 1.3 Surface Scattering

### *1.3.1 Plane Surface*

Surface scattering is the most common scattering in the natural environment. The most basic model would be an infinite perfectly flat surface. Its scattering will concentrate on the specular direction, that is, reflection, which is directly solved as the Fresnel reflection coefficient.

As shown in Figure 1.5, a plane surface has a reflection matrix and a transmission matrix written as

$$\overline{\mathbf{R}} = \begin{bmatrix} R_v & 0 \\ 0 & R_h \end{bmatrix}, \quad \overline{\mathbf{T}} = \begin{bmatrix} T_v & 0 \\ 0 & T_h \end{bmatrix} = \begin{bmatrix} 1+R_v & 0 \\ 0 & 1+R_h \end{bmatrix} \tag{1.42}$$

where $R_v, R_h$ denote the Fresnel coefficients of vertical and horizontal polarization

$$R_v = \frac{\varepsilon_r \cos\theta - \sqrt{\varepsilon_r - \sin^2\theta}}{\varepsilon_r \cos\theta + \sqrt{\varepsilon_r - \sin^2\theta}}, \quad R_h = \frac{\cos\theta - \sqrt{\varepsilon_r - \sin^2\theta}}{\cos\theta + \sqrt{\varepsilon_r - \sin^2\theta}} \tag{1.43}$$

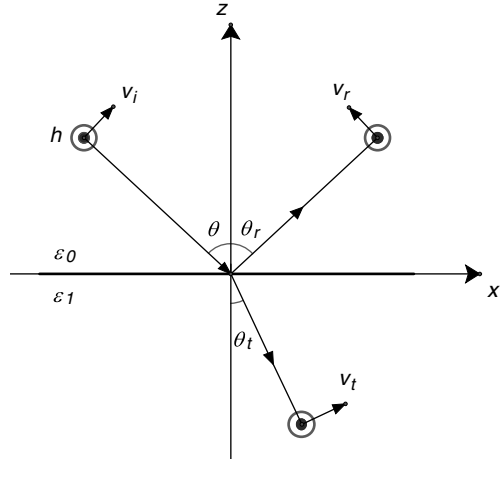



**Figure 1.5** Reflection and transmission of a plane surface

where $\theta$ is the incident angle, and $\varepsilon_r = \varepsilon_1/\varepsilon_0$ is the relative dielectric constant. The reflection angle and transmission angle are related to the incident angle according to Snell's law:

$$\theta_r = \theta, \quad \sqrt{\varepsilon_1}\sin\theta_t = \sqrt{\varepsilon_0}\sin\theta \tag{1.44}$$

For incoherent scattering, the Mueller matrix of plane surface reflection and transmission can be easily derived from Equation 1.17 as

$$\mathbf{R}_{4\times4} = \begin{bmatrix} |R_v|^2 & 0 & 0 & 0 \\ 0 & |R_h|^2 & 0 & 0 \\ 0 & 0 & \mathrm{Re}(R_v R_h^*) & -\mathrm{Im}(R_v R_h^*) \\ 0 & 0 & \mathrm{Im}(R_v R_h^*) & \mathrm{Re}(R_v R_h^*) \end{bmatrix} \tag{1.45}$$

$$\mathbf{T}_{4\times4} = \varepsilon_r \cdot \begin{bmatrix} |T_v|^2 & 0 & 0 & 0 \\ 0 & |T_h|^2 & 0 & 0 \\ 0 & 0 & \dfrac{\cos\theta_t}{\cos\theta}\mathrm{Re}(T_v T_h^*) & -\dfrac{\cos\theta_t}{\cos\theta}\mathrm{Im}(T_v T_h^*) \\ 0 & 0 & \dfrac{\cos\theta_t}{\cos\theta}\mathrm{Im}(T_v T_h^*) & \dfrac{\cos\theta_t}{\cos\theta}\mathrm{Re}(T_v T_h^*) \end{bmatrix} \tag{1.46}$$

Note that the transmission Mueller matrix, Equation 1.46, contains a factor of $\varepsilon_r$ because the Stokes vector includes wave impedance and the transmitted wave and the incident wave are in different media. Since the Mueller matrix is a real matrix, only the real part of $\varepsilon_r$ is used here. Also note that the same letters are used to denote both scattering and Mueller matrix, simply because they are in fact the same reflection or transmission but in different forms.

### *1.3.2 Rough Surface*

In natural environments, most surfaces are randomly rough surfaces, for example, the ground surface, sea surface, and building facets. A randomly rough surface is often described by a random height profile, that is, $z = \xi(x)$ for a 2D rough surface, and $z = \xi(x, y)$ for a 3D rough surface. When calculating rough-surface scattering, the most important entity is the correlation function of the height profile and its Fourier transform, that is, the spectral density function (or spectral function).

A Gaussian rough surface is the most basic type of rough surface. It follows the Gaussian distribution function:

$$p(\xi(x,y)) = \frac{1}{\sqrt{2\pi}\delta}\exp\left[-\xi^2/(2\delta^2)\right] \tag{1.47}$$

Let $\mathbf{r}_{1\perp} \equiv (x_1, y_1)$, the correlation function between $\mathbf{r}_{1\perp}$ and $\mathbf{r}_{2\perp}$, be

$$\delta^2 C(\mathbf{r}_{1\perp}, \mathbf{r}_{2\perp}) = \langle \xi_1(\mathbf{r}_{1\perp})\xi_2(\mathbf{r}_{2\perp})\rangle = \delta^2 \exp\left(-\frac{|\mathbf{r}_{1\perp} - \mathbf{r}_{2\perp}|^2}{\ell^2}\right) \tag{1.48}$$

where the correlation length $\ell$ in both $x$ and $y$ directions is simply assumed to be the same (it can be different as $\ell_x,\ \ell_y$). Then, the joint probability density function can be derived as

$$p(\xi(x,y),\xi(x_1,y_1)) = \frac{1}{2\pi\delta^2\sqrt{1-C^2}}\exp\left[-\frac{\xi^2 - 2C\xi\xi_1 + \xi_1^2}{2\delta^2(1-C^2)}\right] \tag{1.49}$$

$$p\left(\alpha\left[\equiv\frac{\partial}{\partial x}\xi(x,y)\right],\beta\left[\equiv\frac{\partial}{\partial y}\xi(x,y)\right]\right) = \frac{1}{2\pi\delta^2|C''(0)|}\exp\left[-\frac{\alpha^2+\beta^2}{2\delta^2|C''(0)|}\right] \tag{1.50}$$

where $\delta^2|C''(0)|$ is the mean-square surface slope

$$\rho_s^2 = \delta^2|C''(0)| = \frac{2\delta^2}{\ell^2} \tag{1.51}$$

In general, a surface is considered of higher roughness if $\delta$ is larger, $\ell$ is smaller or $\rho_s$ is larger.

The spectral function of a Gaussian surface can be obtained as

$$W(\boldsymbol{\beta}_\perp) = \frac{\delta^2}{(2\pi)^2}\int_{-\infty}^{\infty}\int_{-\infty}^{\infty} d\mathbf{r}_\perp e^{i\boldsymbol{\beta}_\perp\cdot\mathbf{r}_\perp}C(\mathbf{r}_\perp) = \frac{1}{4\pi}\delta^2\ell^2\exp\left[\frac{1}{4}\beta_\perp^2\ell^2\right] \tag{1.52}$$

For different types of rough surfaces, the same scattering model can be applied but with different spectral functions. The most commonly used spectral functions include the Gaussian function, exponential function, and the Pierson–Moskowitz empirical spectrum, which is often used to model the wind-driven sea surface (Fung and Lee, 1982; Huang and Jin, 1995).

The scattering model of a rough surface is illustrated in Figure 1.6. We define the random height profile function as $z = \xi(x,y)$. If a polarized wave $\overline{\mathbf{E}}_i$ is incident in the direction $(\pi-\theta_i,\phi_i)$, the scattered wave $\overline{\mathbf{E}}_s$ in the direction $(\theta_s,\phi_s)$ can be written as

$$\mathbf{E}_s(\mathbf{r}) = \frac{e^{ikr}}{r}\overline{\mathbf{S}}(\theta_s,\phi_s;\theta_i,\phi_i)\cdot\mathbf{E}_i \tag{1.53}$$

Following Huygens' principle (Kong, 2005), Equation 1.53 can be derived as integration of the induced electric and magnetic fields on the rough surface,

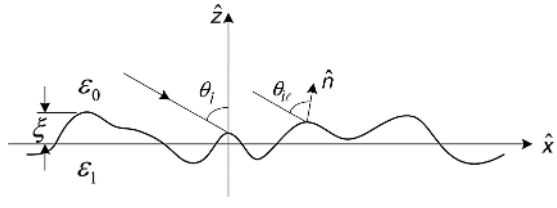



**Figure 1.6** Scattering model of a rough surface

$$\mathbf{E}_s(\mathbf{r}) = \int_A d\boldsymbol{\rho}' \{ i\omega\mu_0 \bar{\mathbf{G}}(\mathbf{r},\mathbf{r}') \cdot [\hat{n} \times \mathbf{H}(\mathbf{r}')] + \nabla \times \bar{\mathbf{G}}(\mathbf{r},\mathbf{r}') \cdot [\hat{n} \times \mathbf{E}(\mathbf{r}')] \} \tag{1.54}$$

where $\overline{\mathbf{G}}(\mathbf{r},\mathbf{r}')$ denotes the dyadic Green function, $\mathbf{E}(\mathbf{r}')$, $\mathbf{H}(\mathbf{r}')$ are the induced electric and magnetic fields at position $\mathbf{r}'(\in S)$, and $\hat{n}$ denotes the local normal vector at position $\mathbf{r}'$, that is

$$\hat{n} = \frac{-\alpha\hat{x} - \beta\hat{y} + \hat{z}}{\sqrt{1+\alpha^2+\beta^2}}, \quad \alpha = \frac{\partial}{\partial x}\xi(x,y), \quad \beta = \frac{\partial}{\partial y}\xi(x,y) \tag{1.55}$$

Under the far-field approximation, this yields

$$\mathbf{E}_s(\mathbf{r}) = \frac{ike^{ikr}}{4\pi r}(\bar{\mathbf{I}} - \hat{k}_s\hat{k}_s) \cdot \int_A d\boldsymbol{\rho}' \{ \hat{k}_s \times [\hat{n} \times \mathbf{E}(\mathbf{r}')] + \eta_0 [\hat{n} \times \mathbf{H}(\mathbf{r}')] \} e^{-i\mathbf{k}_s \cdot \mathbf{r}'} \tag{1.56}$$

Clearly, $\mathbf{E}_s(\mathbf{r})$ and $\mathbf{E}(\mathbf{r}')$, $\mathbf{H}(\mathbf{r}')$ are random. However, the incoherent scattering, that is, the ensemble average of the scattering wave, $\langle |\mathbf{E}_s|^2 \rangle$, is of interest to us, which is further related to the correlation function and spectral function of the rough surface.

Approximate analytical solutions to the problem of rough-surface scattering can be mainly categorized into the Kirchhoff approximation (KA) approach, which is valid for large-scale roughness, the small-perturbation approximation (SPA), suitable for small-scale roughness, the two-scale approximation (TSA) approach, which combines the former two, and the integral equation method (IEM), which are introduced in detail in the following subsections.

### *1.3.3 Kirchhoff Approximation*

If the rough surface fluctuates on a large scale, meaning that its average radius of curvature is far larger than its wavelength, then any portion of the surface can be locally seen as a flat facet and the induced current can be approximated as the equivalent tangential field. The validity condition of KA can be summarized as

$$k_1\ell > 6, \quad k_1\delta > \sqrt{10}/(\cos\theta_i - \cos\theta_s), \quad R_c > \lambda \tag{1.57}$$

where

$$R_c = \delta \sqrt{\frac{2}{\pi} \frac{\partial^4 C(\xi)}{\partial \xi^4}\bigg|_{\xi=0}}$$

denotes the mean radius of curvature, the wavenumber $k_1 = (2\pi/\lambda)\sqrt{\varepsilon_1}$, and $\varepsilon_1$ is the dielectric constant.

For a Gaussian rough surface, this translates to

$$\ell^2 > 2.76\delta\lambda \tag{1.58}$$

Using KA, Equation 1.53 can be derived as

$$\mathbf{E}_s(r) = \frac{ike^{ikr}}{4\pi r} E_0(\bar{\mathbf{I}} - \hat{k}_s\hat{k}_s) \int_A d\boldsymbol{\rho}' \mathbf{F}(\alpha,\beta) e^{i\mathbf{k}_d\cdot\mathbf{r}'} \tag{1.59}$$

where

$$\begin{aligned}\mathbf{F}(\alpha,\beta) = (1+\alpha^2+\beta^2)^{1/2}\{&-(\hat{e}_i\cdot\hat{q}_i)(\hat{n}\cdot\hat{k}_i)(1-R_{h\ell})\hat{q}_i + (\hat{e}_i\cdot\hat{p}_i)(\hat{n}\times\hat{q}_i)(1+R_{v\ell}) \\ &+(\hat{e}_i\cdot\hat{q}_i)[\hat{k}_s\times(\hat{n}\times\hat{q}_i)](1+R_{h\ell}) + (\hat{e}_i\cdot\hat{p}_i)(\hat{n}\cdot\hat{k}_i)(\hat{k}_s\times\hat{q}_i)(1-R_{v\ell})\}\end{aligned} \tag{1.60}$$

$$\mathbf{k}_d \equiv \mathbf{k}_i - \mathbf{k}_s = k_{dx}\hat{x} + k_{dy}\hat{y} + k_{dz}\hat{z} \tag{1.61}$$

The local Fresnel coefficients are

$$R_{h\ell} = \frac{k\cos\theta_{i\ell} - \sqrt{k_1^2 - k^2\sin^2\theta_{i\ell}}}{k\cos\theta_{i\ell} + \sqrt{k_1^2 - k^2\sin^2\theta_{i\ell}}}, \quad R_{v\ell} = \frac{\varepsilon_1 k\cos\theta_{i\ell} - \varepsilon_0\sqrt{k_1^2 - k^2\sin^2\theta_{i\ell}}}{\varepsilon_1 k\cos\theta_{i\ell} + \varepsilon_0\sqrt{k_1^2 - k^2\sin^2\theta_{i\ell}}} \tag{1.62}$$

where $k$, $k_1$ denote the wavenumber in the upper and lower half-spaces, respectively. The local incident angle $\theta_{i\ell}$ is determined by $\cos\theta_{i\ell} = -\hat{n}\cdot\hat{k}_i$.

The integration of $\mathbf{F}(\alpha,\beta)$ can be calculated using the stationary phase method (Tsang *et al.*, 1985; Jin, 1994), that is

$$\mathbf{E}_s(\mathbf{r}) = \frac{ike^{ikr}}{4\pi r} E_0(\bar{\mathbf{I}} - \hat{k}_s\hat{k}_s)\cdot\mathbf{F}(\alpha_0,\beta_0) I \tag{1.63}$$

$$I = \int_A d\boldsymbol{\rho}' \exp(i\mathbf{k}_d\cdot\mathbf{r}'), \quad \mathbf{k}_d \equiv \mathbf{k}_i - \mathbf{k}_s \tag{1.64}$$

where $\alpha_0$, $\beta_0$ denote the stationary phase points, and $I$ in Equation 1.64 is a random term related to the rough surface.

The second-order moment of scattering fields consists of two components: coherent part $\mathbf{E}_m(\mathbf{r})$ (mean-square) and incoherent part $\tilde{\mathbf{E}}(\mathbf{r})$ (variance):

$$\langle|\mathbf{E}_s(\mathbf{r})|^2\rangle = |\mathbf{E}_m(\mathbf{r})|^2 + \langle|\tilde{\mathbf{E}}(\mathbf{r})|^2\rangle \tag{1.65}$$

$$|\mathbf{E}_m(\mathbf{r})|^2 = \frac{k^2|E_0|^2}{16\pi^2 r^2}\left[|\hat{v}_s\cdot\mathbf{F}(\alpha_0,\beta_0)|^2 + |\hat{h}_s\cdot\mathbf{F}(\alpha_0,\beta_0)|^2\right]\cdot|\langle I\rangle|^2 \tag{1.66}$$

$$\langle|\tilde{\mathbf{E}}(\mathbf{r})|^2\rangle = \frac{k^2|E_0|^2}{16\pi^2 r^2}\left[|\hat{v}_s\cdot\mathbf{F}(\alpha_0,\beta_0)|^2 + |\hat{h}_s\cdot\mathbf{F}(\alpha_0,\beta_0)|^2\right]\cdot(\langle II^*\rangle - |\langle I\rangle|^2) \tag{1.67}$$

For a Gaussian rough surface, the random term is calculated as

$$|\langle I\rangle|^2 = \int dx \int dy(2L_x - |x|)(2L_y - |y|)\cdot\exp(-k_{dz}^2\delta^2) = 4\pi^2 A\exp(-k_{dz}^2\delta^2)\delta(k_{dx})\delta(k_{dy}) \tag{1.68}$$

where $2L_x\cdot 2L_y = A$, and $\delta(k_{dx})$, $\delta(k_{dy})$ are the Dirac delta functions.

The coherent part $|\mathbf{E}_m(\mathbf{r})|^2$, however, only exists in the specular direction

$$\begin{aligned} D_I &\equiv \langle II^* \rangle - |\langle I \rangle|^2 \\ &= A \int dx \int dy \{\exp[-k_{dz}^2 \delta^2 (1 - C(\mathbf{r}_\perp))] - \exp(-k_{dz}^2 \delta^2)\} \exp(ik_{dx}x + ik_{dy}y) \end{aligned} \tag{1.69}$$

For a Gaussian rough surface, it can be explicitly derived as

$$D_I = \pi A \sum_{m=1}^{\infty} \frac{(k_{dz}^2 \delta^2)^m}{m!m} \ell^2 \exp\left[-\frac{(k_{dx}^2 + k_{dy}^2)\ell^2}{4m}\right] \exp(-k_{dz}^2 \delta^2) \tag{1.70}$$

Finally, the bistatic scattering coefficient is written as

$$\gamma_{pq}(\hat{k}_s, \hat{k}_i) = \frac{4\pi r^2 \langle |\mathbf{E}_s(\mathbf{r})| \rangle_p}{A \cos\theta_i |E_0|_q^2} = \gamma_{pq}^c(\hat{k}_s, \hat{k}_i) + \gamma_{pq}^{ic}(\hat{k}_s, \hat{k}_i), \quad p, q = v, h \tag{1.71}$$

where superscripts $c$, $ic$ denote the coherent and incoherent parts, respectively, that is

$$\gamma_{pq}^c(\hat{k}_s, \hat{k}_i) = \frac{4\pi |R_{p0}|^2}{\sin\theta_i} \exp(-4k^2\delta^2 \cos^2\theta_i) \delta(\theta_s - \theta_i) \delta(\phi_s - \phi_i) \delta_{pq} \tag{1.72}$$

$$\gamma_{pq}^{ic}(\hat{k}_s, \hat{k}_i) = \frac{k^2}{4\pi A \cos\theta_i} |\hat{p}_s \cdot \mathbf{F}_q(\alpha_0, \beta_0)|^2 D_I \tag{1.73}$$

where $R_{p0}(p = v, h)$ is the Fresnel coefficient of flat surface at incident angle $\theta_i$, and $\delta_{pp} = 1$, $\delta_{pq}(p \neq q) = 0$. Further,

$$|\hat{p}_s \cdot \mathbf{F}_q(\alpha_0, \beta_0)|^2 = \frac{|\bar{k}_d|^4}{k^2 |\hat{k}_i \times \hat{k}_s|^4 k_{dz}^2} f_{pq} \tag{1.74}$$

$$f_{vv} = |(\hat{h}_s \cdot \hat{k}_i)(\hat{h}_i \cdot \hat{k}_s) R_{h\ell} + (\hat{v}_s \cdot \hat{k}_i)(\hat{v}_i \cdot \hat{k}_s) R_{v\ell}|^2 \tag{1.75a}$$

$$f_{hh} = |(\hat{v}_s \cdot \hat{k}_i)(\hat{v}_i \cdot \hat{k}_s) R_{h\ell} + (\hat{h}_s \cdot \hat{k}_i)(\hat{h}_i \cdot \hat{k}_s) R_{v\ell}|^2 \tag{1.75b}$$

$$f_{vh} = |(\hat{v}_s \cdot \hat{k}_i)(\hat{h}_i \cdot \hat{k}_s) R_{h\ell} - (\hat{h}_s \cdot \hat{k}_i)(\hat{v}_i \cdot \hat{k}_s) R_{v\ell}|^2 \tag{1.75c}$$

$$f_{hv} = |(\hat{h}_s \cdot \hat{k}_i)(\hat{v}_i \cdot \hat{k}_s) R_{h\ell} - (\hat{v}_s \cdot \hat{k}_i)(\hat{h}_i \cdot \hat{k}_s) R_{v\ell}|^2 \tag{1.75d}$$

where

$$\hat{n} = \frac{k_{dx}/k_{dz}\hat{x} + k_{dy}/k_{dz}\hat{y} + \hat{z}}{(1 + k_{dx}^2/k_{dz}^2 + k_{dy}^2/k_{dz}^2)^{1/2}} \tag{1.76}$$

Given $k \to \infty$, the bistatic scattering coefficient can be simplified to

$$\gamma_{pq}(\hat{k}_s, \hat{k}_i) = \frac{\pi |\bar{k}_d|^4}{\cos\theta_i |\hat{k}_i \times \hat{k}_s|^4 k_{dz}^4} f_{pq} p\left(-\frac{k_{dx}}{k_{dz}}, -\frac{k_{dy}}{k_{dz}}\right) \tag{1.77}$$

Using Equation 1.50, the bistatic scattering coefficient of Equation 1.77 is written as

$$\gamma_{pq}(\hat{k}_s, \hat{k}_i) = \frac{|\bar{k}_d|^4}{\cos\theta_i |\hat{k}_i \times \hat{k}_s|^4 \frac{dz}{k}^4} f_{pq} \frac{1}{2\delta^2 |C''(0)|} \exp\left[-\frac{k_{dx}^2 + k_{dy}^2}{2k_{dz}^2 \delta^2 |C''(0)|}\right] \tag{1.78}$$

and the backscattering coefficient is calculated as

$$\sigma_{hh}(\theta_i) = \sigma_{vv}(\theta_i) = \frac{|R(0)|^2}{\cos^4\theta_i 2\delta^2 |C''(0)|} \exp\left(-\frac{\tan^2\theta_i}{2\delta^2 |C''(0)|}\right) \tag{1.79}$$

$$\sigma_{hv}(\theta_i) = \sigma_{vh}(\theta_i) = 0 \tag{1.80}$$

where $R(0)$ is the Fresnel coefficient of the flat surface at zero degree incidence. Note that the term $\delta^2 |C''(0)|$ is in fact the square of the average slope. In the case of a Gaussian correlation function, we have $|C''(0)| = 2/\ell^2$. Some of the terms related to wavenumber can be expanded as

$$k_d^2 = 2k^2[1 + \cos\theta_i \cos\theta_s - \sin\theta_i \sin\theta_s \cos(\phi_s - \phi_i)] \tag{1.81}$$

$$k_{dz}^2 = k^2(\cos\theta_i + \cos\theta_s)^2 \tag{1.82}$$

$$|\hat{k}_i \times \hat{k}_s|^2 = 1 - [\cos\theta_i \cos\theta_s - \sin\theta_i \sin\theta_s \cos(\phi_s - \phi_i)]^2 \tag{1.83}$$

Likewise, the transmission coefficients under KA can be derived, for which readers are referred to Tsang, Kong, and Shin (1985, p. 89).

### *1.3.4 Small-Perturbation Approximation*

SPA, also referred to as the small-perturbation method (SPM), is valid when the roughness is very small compared to the wavelength (Rice, 1963), that is, the root-mean-square height $\delta \ll \lambda$ and mean slope $s$ is comparable to $k\delta$, which can be represented by the following inequalities (Chen and Fung, 1988):

$$k_1 \ell < 3, \quad k_1 \delta < 0.3, \quad s < 0.3 \tag{1.84}$$

From Huygens' principle, Equation 1.53, let us expand the incident field $\mathbf{E}_i$, the scattered field $\mathbf{E}_s$, and the surface field $\mathbf{E}(\mathbf{r}')$ on a rough surface into a perturbation series of $k\xi$. The zero-order term of the scattered field is the specular reflection of the plane surface. The first-order term is the incoherent part of the rough-surface scattering. Higher orders corresponds to multiple scatterings occurring on the rough surface. For detailed derivation of the SPA

solution, readers are referred to the literature, such as Bass and Fuks (1979), Ulaby, Moore, and Fung (1982), and Tsang, Kong, and Shin (1985).

The first-order SPA bistatic scattering coefficient can be written as

$$\gamma_{pq}^{(\mathrm{SPA1})}(\hat{k}_s, \hat{k}_i) = 16\pi k^4 \cos^2\theta_s \cos\theta_i F_{pq} W(|\mathbf{k}_{\rho s} - \mathbf{k}_{\rho i}|) \tag{1.85}$$

where $W(|\mathbf{k}_{d\perp}|)$ is the spectral function and

$$F_{hh} = \left| \frac{k_1^2 - k^2}{(k_{zs} + k_{1zs})(k_{zi} + k_{1zi})} \right| \cos^2(\phi_s - \phi_i) \tag{1.86}$$

$$F_{vv} = \left| \frac{k_1^2 - k^2}{(k_1^2 k_{zs} + k^2 k_{1zs})(k_1^2 k_{zi} + k^2 k_{1zi})} \left[k_1^2 k^2 \sin\theta_s \sin\theta_i - k^2 k_{1zs} k_{1zi} \cos(\phi_s - \phi_i)\right] \right|^2 \tag{1.87}$$

$$F_{hv} = \left| \frac{k k_{1zi}(k_1^2 - k^2)}{(k_1^2 k_{zi} + k^2 k_{1zi})(k_{zs} + k_{1zs})} \right|^2 \sin^2(\phi_s - \phi_i) \tag{1.88}$$

$$F_{vh} = \left| \frac{k k_{1zs}(k_1^2 - k^2)}{(k_1^2 k_{zs} + k^2 k_{1zs})(k_{zi} + k_{1zi})} \right|^2 \sin^2(\phi_s - \phi_i) \tag{1.89}$$

For a Gaussian rough surface, it can be further expanded as

$$\gamma_{pq}^{(\mathrm{SPA1})}(\hat{k}_s, \hat{k}_i) = 4k^4 \cos^2\theta_s \cos\theta_i \delta^2 \ell^2 f_{pq} \exp\left(-\frac{1}{4} k_{d\rho}^2 \ell^2\right) \tag{1.90}$$

$$k_{d\rho}^2 = k_{dx}^2 + k_{dy}^2 = k^2[\sin^2\theta_s + \sin^2\theta_i - 2\sin\theta_s \sin\theta_i \cos(\phi_s - \phi_i)] \tag{1.91}$$

While in the backscattering direction, it simplifies to

$$F_{hh}^B = \left| \frac{k_{zi} - k_{1zi}}{k_{zi} + k_{1zi}} \right|^2 = |R_{h0}|^2 \tag{1.92}$$

$$F_{vv}^B = \left| \frac{(k_1^2 - k^2)(k_1^2 k^2 \sin^2\theta_i + k^2 k_{1zi}^2)}{(k_1^2 k_{zi} + k^2 k_{1zi})^2} \right|^2 \tag{1.93}$$

$$F_{vh}^B = F_{hv}^B = 0 \tag{1.94}$$

where the superscript $B$ denotes backscattering. Hence, the backscattering coefficient can be written as

$$\sigma_{hh}^{(\mathrm{SPA1})} = 16\pi k^4 \cos^4\theta_i |R_{h0}|^2 W(2k\sin\theta_i) \tag{1.95}$$

$$\sigma_{vv}^{(\mathrm{SPA1})} = 16\pi k^4 \cos^4\theta_i W(2k\sin\theta_i) \left| \frac{(k_1^2 - k^2)(k_1^2 k^2 \sin^2\theta_i + k^2 k_{1zi}^2)}{(k_1^2 k_{zi} + k^2 k_{1zi})^2} \right|^2 \tag{1.96}$$

$$\sigma_{vh}^{(\mathrm{SPA1})} = \sigma_{hv}^{(\mathrm{SPA1})} = 0 \tag{1.97}$$

For a Gaussian rough surface, this yields

$$\sigma_{hh}^{(\mathrm{SPA1})} = 4k^4\delta^2\ell^2\cos^4\theta_i|R_{h0}|^2\exp(-k^2\ell^2\sin^2\theta_i) \tag{1.98}$$

$$\sigma_{vv}^{(\mathrm{SPA1})} = 4k^4\delta^2\ell^2\cos^4\theta_i\exp(-k^2\ell^2\sin^2\theta_i)\left|\frac{(k_1^2-k^2)(k_1^2k^2\sin^2\theta_i+k^2k_{1zi}^2)}{(k_1^2k_{zi}+k^2k_{1zi})^2}\right|^2 \tag{1.99}$$

Note that the term $|R_{h0}|^2$ is the horizontal-polarization Fresnel reflection coefficient.

Interestingly, the factor in $\sigma_{vv}^{(\mathrm{SPA1})}$ can also be written as

$$\left|\frac{(k_1^2-k^2)(k_1^2k^2\sin^2\theta_i+k^2k_{1zi}^2)}{(k^2k_{zi}+k^2k_{1zi})^2}\right|^2 = \left|R_{v0}+\frac{(k_1^2-k^2)T_{v0}^2\sin^2\theta_i}{2k_1^2\cos^2\theta_i}\right|^2 \tag{1.100}$$

where $R_{v0}$ and $T_{v0}$ denote the vertically polarized Fresnel reflection coefficient and Fresnel transmission coefficient, respectively.

Clearly, the first-order SPA solution has no cross-polarization contribution: $\sigma_{vv}^{(\mathrm{SPA1})} \neq \sigma_{hh}^{(\mathrm{SPA1})}$, $\sigma_{vh}^{(\mathrm{SPA1})} = \sigma_{hv}^{(\mathrm{SPA1})} = 0$. However, $\sigma_{hv}^{(\mathrm{SPA2})}$, $\sigma_{vh}^{(\mathrm{SPA2})} \neq 0$ for the second- or higher-order solutions (Tsang, Kong, and Shin, 1985).

### *1.3.5 Two-Scale Approximation*

In reality, natural surface roughness exists at different scales and therefore cannot be dealt with by either the KA or SPA approach only. The two-scale approximation (TSA) approach is a simple combination of KA and SPA (Wu and Fung, 1972; Jin, 1994). As illustrated in Figure 1.7, the basic assumption for the TSA model is that there is small roughness riding on top of a large fluctuation.

Based on the independent KA and SPA solutions, the TSA combines the two after corresponding modifications. The KA scattering coefficient has to be modified to take into account the dimming effect by small roughness. On the other hand, the SPA solution has to be modified to take into account the local slope.

The TSA backscattering coefficient consists of two parts:

$$\sigma_{pp}(\hat{k}_i) = \sigma_{pp}^{\mathrm{KA}}(\hat{k}_i) + \langle\sigma_{pp}^{\mathrm{SPA}}(\hat{k}_i)\rangle \tag{1.101}$$

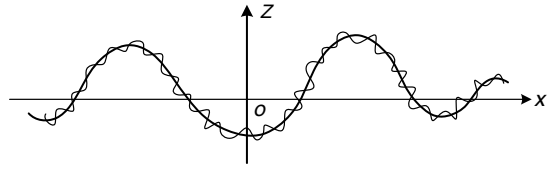



**Figure 1.7** Two-scale model: small-scale roughness riding on large-scale fluctuation

The TSA bistatic coefficient is written as

$$\gamma_{pp}(\hat{k}_s, \hat{k}_i) = \gamma_{pp}^{\mathrm{KA}}(\hat{k}_s, \hat{k}_i) + \langle \gamma_{pp}^{\mathrm{SPA}}(\hat{k}_{s\ell}, \hat{k}_{i\ell}) \rangle \tag{1.102}$$

The second term represents the ensemble average of the SPA solution over the distribution of local slope caused by large-scale fluctuation, that is

$$\begin{aligned} \langle \gamma_{pq}^{(\mathrm{SPA1})}(\hat{k}_{s\ell}, \hat{k}_{i\ell}) \rangle = & \int_{-\cot\theta_2}^{\infty} d\xi_y \int_{-\cot\theta_1}^{\infty} d\xi_x \; \gamma_{pq}^{(\mathrm{SPA1})}(\hat{k}_{s\ell}, \hat{k}_{i\ell}) \\ & [1 + (\xi_x \cos\phi_i + \xi_y \sin\phi_i)\tan\theta_i] p(\xi_{x'}, \xi_{y'}) \end{aligned} \tag{1.103}$$

where $\cot\theta_1 = \cot\theta_i/\cos\phi_i$, $\cot\theta_2 = \cot\theta_i/\sin\phi_i$ is included to account for the self-shadowing effect. Let $\phi_i = 0$, then the integration ranges of $d\xi_x, d\xi_y$ become $(-\cot\theta_i, \infty), (-\infty, \infty)$, respectively. $P(\xi_{x'}, \xi_{y'})$ is the probability distribution function of local slope $(\xi_{x'}, \xi_{y'})$, which is defined as

$$\xi_{x'} \equiv \frac{\partial \xi}{\partial x'} = \xi_x \cos\phi_0 + \xi_y \sin\phi_0, \quad \xi_{y'} \equiv \frac{\partial \xi}{\partial y'} = \xi_y \cos\phi_0 - \xi_x \sin\phi_0 \tag{1.104}$$

Then, the local coordinates $(\hat{x}_\ell, \hat{y}_\ell, \hat{z}_\ell)$ relate to global coordinates $(\hat{x}', \hat{y}', \hat{z})$ as

$$\begin{bmatrix} \hat{x}_\ell \\ \hat{y}_\ell \\ \hat{z}_\ell \end{bmatrix} = \begin{bmatrix} a_{11} & a_{12} & a_{13} \\ a_{21} & a_{22} & a_{23} \\ a_{31} & a_{32} & a_{33} \end{bmatrix} \cdot \begin{bmatrix} \hat{x}' \\ \hat{y}' \\ \hat{z} \end{bmatrix} \tag{1.105}$$

where

$$\begin{aligned} & a_{11} = \cos\theta_n \cos\phi_n, \; a_{12} = -\cos\theta_n \sin\phi_n, \; a_{13} = \sin\theta_n \\ & a_{21} = \sin\phi_n, \; a_{22} = \cos\phi_n, \; a_{23} = 0 \\ & a_{31} = -\sin\theta_n \cos\phi_n, \; a_{32} = \sin\theta_n \sin\phi_n, \; a_{33} = \cos\theta_n \end{aligned}$$

Furthermore, the local angles and local slopes are written as

$$\begin{aligned} \cos\theta_n = (1 + \xi_{x'}^2 + \xi_{y'}^2)^{1/2} = (1 + \xi_x^2 + \xi_y^2)^{1/2}, \; \tan\phi_n = \xi_{y'}/\xi_{x'} \\ \xi_{x'} = (\partial\xi/\partial\rho')(\partial\rho'/\partial x') = \tan\theta_n \cos\phi_n \\ \xi_{y'} = (\partial\xi/\partial\rho')(\partial\rho'/\partial y') = \tan\theta_n \sin\phi_n \end{aligned}$$

Scattering from a randomly rough sea surface using an application of the TSA model can be found in Huang and Jin (1995).

### *1.3.6 Integral Equation Method*

In practice, the KA is often used in circumstances of high frequency and small incident angle ($<20^\circ$), while the SPA is suitable for cases where the frequency is low and the

incident angle is large (20°–84°). The TSA combines the two types of scattering independently and thus is still limited by their respective constraints. Fung (1994) developed the integral equation method (IEM), which introduces a complementary field into the KA framework and takes into account the scattering caused by rapid fluctuations. Most of this book will employ the IEM solution to rough-surface scattering. Its validity condition is written as

$$k\delta \cdot k\ell < 1.2\sqrt{\varepsilon_1} \tag{1.106}$$

The Mueller matrix form of the IEM rough-surface scattering is written as (Fung, 1994)

$$\overline{\mathbf{M}}(\theta_s,\phi_s;\pi-\theta_i,\phi_i)=\begin{bmatrix} \langle|S_{vv}|^2\rangle & \langle|S_{vh}|^2\rangle & \mathrm{Re}\langle S_{vv}S_{vh}^*\rangle & -\mathrm{Im}\langle S_{vv}S_{vh}^*\rangle \\ \langle|S_{hv}|^2\rangle & \langle|S_{hh}|^2\rangle & \mathrm{Re}\langle S_{hv}S_{hh}^*\rangle & -\mathrm{Im}\langle S_{hv}S_{hh}^*\rangle \\ 2\mathrm{Re}\langle S_{vv}S_{hv}^*\rangle & 2\mathrm{Re}\langle S_{vh}S_{hh}^*\rangle & \mathrm{Re}\langle S_{vv}S_{hh}^*+S_{vh}S_{hv}^*\rangle & \mathrm{Im}\langle S_{vh}S_{hv}^*-S_{vv}S_{hh}^*\rangle \\ 2\mathrm{Im}\langle S_{vv}S_{hv}^*\rangle & 2\mathrm{Im}\langle S_{vh}S_{hh}^*\rangle & \mathrm{Im}\langle S_{vv}S_{hh}^*+S_{vh}S_{hv}^*\rangle & \mathrm{Re}\langle S_{vv}S_{hh}^*-S_{vh}S_{hv}^*\rangle \end{bmatrix} \tag{1.107}$$

where

$$\langle S_{pq}S_{rs}^*\rangle=\frac{k^2}{8\pi}\exp\left[-\delta^2(k_{zi}^2+k_{zs}^2)\right]\sum_{n=1}^{\infty}\delta^{2n}(I_{pq}^n I_{rs}^{n*})\frac{W^{(n)}(k_{dx},k_{dy})}{n!},\quad p,q,r,s=v,h \tag{1.108}$$

$$I_{pq}^n=(k_{zi}+k_{zs})^n f_{pq}\exp(-\delta^2 k_{zi}k_{zs})+\frac{(k_{zs})^n F_{pq}(-k_{xi},-k_{yi})+(k_{zi})^n F_{pq}(-k_{xs},-k_{ys})}{2} \tag{1.109}$$

The KA coefficients are

$$\begin{aligned} f_{vv}&=\frac{2R_v}{\cos\tilde{\theta}_i+\cos\theta_s}\left[\sin\tilde{\theta}_i\sin\theta_s-(1+\cos\tilde{\theta}_i\cos\theta_s)\cos(\varphi_s-\varphi_i)\right] \\ f_{hh}&=\frac{2R_h}{\cos\tilde{\theta}_i+\cos\theta_s}\left[\sin\tilde{\theta}_i\sin\theta_s-(1+\cos\tilde{\theta}_i\cos\theta_s)\cos(\varphi_s-\varphi_i)\right] \\ f_{hv}&=(R_h-R_v)\sin(\varphi_s-\varphi_i),\ f_{vh}=(R_v-R_h)\sin(\varphi_i-\varphi_s) \end{aligned} \tag{1.110}$$

and the complementary field coefficients are

$$\begin{aligned} F_{vv}&=-(cu_v-qt_v/\varepsilon_r)(t_v c_d+u_v\varepsilon_r c_1)+(v_v^2-ct_v u_v/q)c_2^s \\ F_{hh}&=(cu_h-qt_h)(t_h c_d+u_h c_1)-(v_h^2-ct_h u_h/q)c_2^s \\ F_{hv}&=(cu-qt/\varepsilon_r)(t/c_s+u\varepsilon_r/q)s_d+(u^2-ctu/q)s^2 s_d \\ F_{vh}&=(ct-qu)(u/c_s+tq)s_d+(t^2-ctu/q)s^2 s_d \\ F_{vv}^s&=-(c_s u_v-q_s t_v/\varepsilon_r)(t_v c_d+u_v\varepsilon_r c_1^s)+(t_v^2-c_s t_v u_v/q_s)c_2^s \\ F_{hh}^s&=(c_s u_h-q_s t_h)(t_h c_d+u_h c_1^s)-(t_h^2-c_s t_h u_h/q_s)c_2^s \\ F_{hv}^s&=-(c_s t-q_s u)(u/c_s+t/q_s)s_d-(u^2-c_s tu/q_s)s_s^2 s_d \\ F_{vh}^s&=-(c_s u-q_s t/\varepsilon_r)(t/c_s+u\varepsilon_r/q_s)s_d-(t^2-c_s tu/q_s)s_s^2 s_d \end{aligned} \tag{1.111}$$

where the numerous symbols employed are defined as

$$\begin{aligned}
&s=\sin\tilde{\theta}_i,\ \ s_s=\sin\theta_s,\ \ s_d=\sin(\varphi_s-\varphi_i)\\
&c=\cos\tilde{\theta}_i,\ \ c_s=\cos\theta_s,\ \ c_d=\cos(\varphi_s-\varphi_i)\\
&q=\sqrt{\varepsilon_r-\sin^2\tilde{\theta}_i},\ \ q_s=\sqrt{\varepsilon_r-\sin^2\theta_s}\\
&c_1=\frac{c_d-ss_s}{qc_s},\ \ c_1^s=\frac{c_d-ss_s}{q_sc},\ \ c_2=s\frac{s_s-sc_d}{c_s},\ \ c_2^s=s_s\frac{s-s_sc_d}{c}\\
&t_v=1+R_v,\ \ t_h=1+R_h,\ \ t=1+(R_v-R_h)/2\\
&u_v=1-R_v,\ \ u_h=1-R_h,\ \ u=1-(R_v-R_h)/2\\
&k_x=k\sin\tilde{\theta}_i\cos\varphi_i,\ \ k_y=k\sin\tilde{\theta}_i\sin\varphi_i,\ \ k_z=k\cos\tilde{\theta}_i\\
&k_{sx}=k\sin\theta_s\cos\varphi_s,\ \ k_{sy}=k\sin\theta_s\sin\varphi_s,\ \ k_{sz}=k\cos\theta_s
\end{aligned}\tag{1.112}$$

For rough-surface transmission, the Mueller matrix $\overline{\mathbf{M}}(\theta_t,\phi_t;\pi-\theta_i,\phi_i)$ has exactly the same form as for scattering but with its elements replaced by (Fung, 1994)

$$\langle S_{pq}S_{rs}^*\rangle=\frac{k_1^2}{8\pi}\exp\left[-\delta^2(k_{zi}^2+k_{zt}^2)\right]\sum_{n=1}^{\infty}\delta^{2n}(I_{pq}^nI_{rs}^{n*})\frac{W^{(n)}(k_{1dx},k_{1dy})}{n!},\qquad p,q,r,s=v,h \tag{1.113}$$

$$I_{pq}^n=(k_{zi}+k_{zt})^nf_{1pq}\exp(-\delta^2k_{zi}k_{zt})+\frac{(-k_{zt})^nF_{1pq}(-k_{xi},-k_{yi})+(k_{zi})^nF_{1pq}(-k_{xt},-k_{yt})}{2} \tag{1.114}$$

$$\begin{aligned}
f_{vv}^t&=Au_v+Bt_v,\ \ f_{hh}^t=-Bt_h-Au_h\\
f_{hv}^t&=Cu+s_ft,\ \ f_{vh}^t=s_fu+Ct\\
F_{vv}^t&=-(cu_v-qt_v/\varepsilon_r)(t_vc_f+u_vA_1)-(v_v^2-ct_vu_v/q)A_2\\
F_{hh}^t&=(cu_h-qt_h)(t_hc_f+u_hA_1)m/\varepsilon_r+(v_h^2-ct_hu_h/q)A_2m/\varepsilon_r
\end{aligned}\tag{1.115}$$

$$\begin{aligned}
F_{hv}^t&=(cu-qt/\varepsilon_r)(um/q-t/c_t)s_f-(u^2-ctu/q)s^2s_f/m\\
F_{vh}^t&=(ct-qu)(tm/q-t/c_t)s_fm/\varepsilon_r-(t^2-ctu/q)s^2s_f/m\\
F_{vv}^{tt}&=-(q_tu_v-c_tmt_v/\varepsilon_r)(t_vc_f+u_vA_1^t)-(c_tt_v^2/q_t-t_vu_v/m)A_2^t\\
F_{hh}^{tt}&=(q_tu_h-c_tmt_h)(t_hc_f+u_hA_1^t)m/\varepsilon_r+(c_tt_h^2/q_t-t_hu_h/m)mA_2^t\\
F_{hv}^{tt}&=(q_tt-c_tmu)(t/q_t-u/c)s_f/m+(c_tmu^2/q_t-tu)ms_t^2s_f\\
F_{vh}^{tt}&=(q_tu-c_tmt/\varepsilon_r)(u/q_t-t/c)s_f+(c_tmt^2/q_t-tu)s_t^2s_f
\end{aligned}\tag{1.116}$$

and

$$\begin{aligned}
s&=\sin\tilde{\theta}_i,\ \ s_t=\sin\tilde{\theta}_t,\ \ s_f=\sin\varphi_t,\ \ c=\cos\tilde{\theta}_i,\ \ c_t=\cos\tilde{\theta}_t,\ \ c_f=\cos\varphi_t\\
m&=\sqrt{\varepsilon_r},\ \ q_t=\sqrt{1-\varepsilon_r\sin^2\tilde{\theta}_t}\\
A&=(c+sZ_x)c_f+s_fsZ_y,\ \ B=c_tc_f+Z_xs_t\\
C&=c_ts_f(c+sZ_x)+Z_y(s_tc-sc_tc_f)\\
Z_x&=\frac{ms_tc_f-s}{mc_t-c},\ \ Z_y=\frac{ms_ts_f}{mc_t-c}\\
A_1&=\frac{s_ts-mc_f}{c_tmc_t},\ \ A_2=\frac{s(s_t-sc_f/m)}{c_t},\ \ A_1^t=\frac{ms_ts-c_f}{q_tc},\ \ A_2^t=\frac{s_t(s-s_tc_fm)}{c}\\
t_v&=1+R_v,\ \ t_h=1+R_h,\ \ t=1+(R_v-R_h)/2\\
u_v&=1-R_v,\ \ u_h=1-R_h,\ \ u=1-(R_v-R_h)/2\\
k_x&=k\sin\tilde{\theta}_i\cos\varphi_i,\ \ k_y=k\sin\tilde{\theta}_i\sin\varphi_i,\ \ k_z=k\cos\tilde{\theta}_i\\
k_{tx}&=km\sin\tilde{\theta}_t\cos\varphi_t,\ \ k_{ty}=km\sin\tilde{\theta}_t\sin\varphi_t,\ \ k_{sz}=km\cos\tilde{\theta}_t
\end{aligned}\tag{1.117}$$

### 1.3.7 Tilted Surface or Oriented Object

A rough surface may be tilted as a result of topographic fluctuation. Terrain objects or building surfaces may have different orientations in common global coordinates. Thus, a general method of coordinate conversion would be useful in adapting canonical scattering models for a tilted surface or oriented object.

As shown in Figure 1.8, the orientation of local coordinates $(\hat{x}', \hat{y}', \hat{z}')$ is defined by three Euler angles $\alpha, \beta, \gamma$ (Tsang, Kong, and Shin, 1985; Jin, 1994). Through three steps of rotation, $(\hat{x}', \hat{y}', \hat{z}')$ can be aligned with the global coordinates $(\hat{x}, \hat{y}, \hat{z})$: that is, first rotate along $\hat{z}'$ by angle $\alpha$ so that $\hat{y}'$ is located in the $xoy$ plane ($\hat{y}'$ becomes $\hat{y}''$); then rotate along $\hat{z}'$ by angle $\beta$ so that $\hat{y}''$ is overlapped with $\hat{z}$; finally, rotate along $\hat{z}$ by angle $\gamma$ so that $\hat{y}''$ is overlapped with $\hat{y}$, so do the other two axes.

The coordinate conversion can be expressed in matrix form as

$$
\begin{aligned}
&[x' \quad y' \quad z']^{\mathrm{T}} = \overline{\mathbf{T}} \cdot [x \quad y \quad z]^{\mathrm{T}} \\
&T_{11} = \cos\gamma\cos\beta\cos\alpha - \sin\gamma\sin\alpha, \\
&T_{12} = -\sin\gamma\cos\beta\cos\alpha - \cos\gamma\sin\alpha, \quad T_{13} = \sin\beta\cos\alpha \\
&T_{21} = \cos\gamma\cos\beta\sin\alpha + \sin\gamma\cos\alpha, \\
&T_{22} = -\sin\gamma\cos\beta\sin\alpha + \cos\gamma\cos\alpha, \quad T_{23} = \sin\beta\sin\alpha \\
&T_{31} = -\cos\gamma\sin\beta, \quad T_{32} = \sin\gamma\sin\beta, \quad T_{33} = \cos\beta
\end{aligned}
\tag{1.118}
$$

If the scatterer has rotational symmetry along $\hat{z}'$, without loss of generality let $\alpha = 0$ and it is simplified to

$$
\overline{\mathbf{T}} = \begin{bmatrix} \cos\gamma\cos\beta & -\sin\gamma\cos\beta & \sin\beta \\ \sin\gamma & \cos\gamma & 0 \\ -\cos\gamma\sin\beta & \sin\gamma\sin\beta & \cos\beta \end{bmatrix} \tag{1.119}
$$

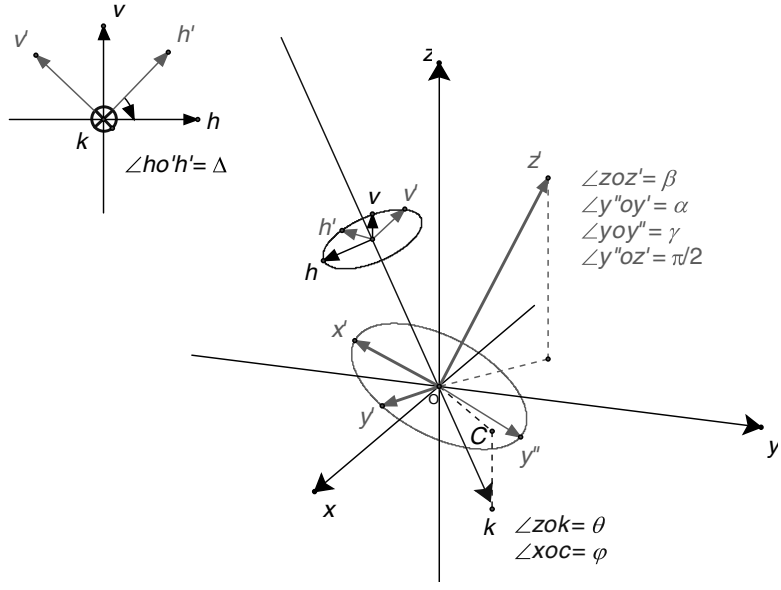



**Figure 1.8** Global coordinates and local coordinates

In addition, the wave propagation vector $\hat{k}(\theta,\phi)$ defined in $(\hat{x},\hat{y},\hat{z})$ and the vector $\hat{k}(\theta',\phi')$ defined in $(\hat{x}',\hat{y}',\hat{z}')$ has the following conversion:

$$\begin{aligned}
&\theta' = \cos^{-1}(-\sin\theta\cos\varphi\sin\beta\cos\gamma + \sin\theta\sin\varphi\sin\gamma\sin\beta + \cos\theta\cos\beta)\\
&\cos\varphi'\sin\theta' = \sin\theta\cos\varphi\cos\beta\cos\gamma - \sin\theta\sin\varphi\cos\beta\sin\gamma + \cos\theta\sin\beta\\
&\mathrm{sgn}(\varphi') = \mathrm{sgn}(\sin\theta\cos\varphi\sin\gamma + \sin\theta\sin\varphi\cos\gamma)
\end{aligned} \tag{1.120}$$

Note that the polarization basis defined in two coordinate systems also differs by a certain angle $\Delta$. Here, it is defined as the angle required to rotate $(\hat{v}',\hat{h}')$ clockwise (as seen from the $\hat{k}$ direction) to $(\hat{v},\hat{h})$, that is

$$\begin{cases}
\cos\Delta = \hat{h}'\cdot\hat{h} = (\hat{k}\times\hat{z}')\cdot(\hat{k}\times\hat{z}) / |\hat{z}'\times\hat{k}||\hat{z}\times\hat{k}| = \dfrac{\cos\beta - \cos\theta\cos\theta'}{\sin\theta\sin\theta'}\\
\mathrm{sgn}(\Delta) = \mathrm{sgn}[(\hat{h}'\times\hat{h})\cdot\hat{k}] = \mathrm{sgn}[\sin(\varphi+\gamma)]
\end{cases} \tag{1.121}$$

Now we can conclude the coordinate conversions of the scattering matrix $\overline{\mathbf{S}}(\theta_s,\varphi_s;\theta_i,\varphi_i)$, $\overline{\mathbf{S}'}(\theta'_s,\varphi'_s;\theta'_i,\varphi'_i)$ and the Mueller matrix $\overline{\mathbf{M}}(\theta_s,\varphi_s;\theta_i,\varphi_i)$, $\overline{\mathbf{M}'}(\theta'_s,\varphi'_s;\theta'_i,\varphi'_i)$:

$$\overline{\mathbf{S}}(\theta_s,\varphi_s;\theta_i,\varphi_i) = \overline{\mathbf{U}}(\Delta_s)\cdot\overline{\mathbf{S}'}(\theta'_s,\varphi'_s;\theta'_i,\varphi'_i)\cdot\overline{\mathbf{U}}^{-1}(\Delta_i) \tag{1.122}$$

$$\overline{\mathbf{M}}(\theta_s,\varphi_s;\theta_i,\varphi_i) = \overline{\mathbf{U}}_{4\times4}(\Delta_s)\cdot\overline{\mathbf{M}'}(\theta'_s,\varphi'_s;\theta'_i,\varphi'_i)\cdot\overline{\mathbf{U}}_{4\times4}^{-1}(\Delta_i) \tag{1.123}$$

where the polarization basis rotation matrix is given as (Xu and Jin, 2006)

$$\overline{\mathbf{U}}(\Delta) = \begin{bmatrix} \cos\Delta & \sin\Delta \\ -\sin\Delta & \cos\Delta \end{bmatrix} \tag{1.124}$$

$$\overline{\mathbf{U}}_{4\times4}(\Delta) = \begin{bmatrix} \cos^2\Delta & \sin^2\Delta & \frac{1}{2}\sin 2\Delta & 0 \\ \sin^2\Delta & \cos^2\Delta & -\frac{1}{2}\sin 2\Delta & 0 \\ -\sin 2\Delta & \sin 2\Delta & \cos 2\Delta & 0 \\ 0 & 0 & 0 & 1 \end{bmatrix} \tag{1.125}$$

With the above equations, we can always calculate the new scattering matrix and Mueller matrix of a scatterer after being rotated to a new orientation.

## References

Bass, F.G. and Fuks, I.M. (1979) *Wave Scattering from Statistically Rough Surface*, Pergamon, New York.

Chen, M.F. and Fung, A.K. (1988) A numerical study of the regions of validity of Kirchhoff and small perturbed rough surface scattering models. *Radio Science*, **24** (2), 163–170.

Fung, A.K. (1994) *Microwave Scattering and Emission Models and Their Applications*, Artech House, Norwood, MA.

Fung, A.K. and Lee, K.K. (1982) A semi-empirical sea-spectrum model for scattering coefficient estimation. *IEEE Journal of Oceanic Engineering*, **7** (4), 166–176.

Huang, X. and Jin, Y.Q. (1995) Scattering and emission from two-scale randomly rough sea surface with foam scatterers. *IEE Proceedings H – Microwaves, Antennas, and Propagation*, **142** (2), 109–114.

Ishimaru, A. (1978) *Wave Propagation and Scattering in Random Media*, Academic Press, New York.

Ishimaru, A. (1991) *Electromagnetic Wave Propagation, Radiation, and Scattering*, Prentice-Hall, Englewood Cliffs, NJ.

Jin, Y.Q. (1994) *Electromagnetic Scattering Modelling for Quantitative Remote Sensing*, World Scientific, Singapore.

Karam, M.A. and Fung, A.K. (1988) Electromagnetic scattering from a layer of finite-length randomly oriented dielectric circular cylinders. *International Journal of Remote Sensing*, **9** (6), 1109–1134.

Kong, J.A. (2005) *Electromagnetic Wave Theory*, EMW Publishing, Cambridge, MA.

Rice, S.O. (1963) *Reflection of Electromagnetic Waves by Slightly Rough Surfaces*, Interscience, New York.

Tsang, L., Kong, J.A., and Shin, B. (1985) *Theory of Microwave Remote Sensing*, John Wiley & Sons, Inc., New York.

Ulaby, F.T., Moore, R.K., and Fung, A.K. (1982) *Microwave Remote Sensing: Active and Passive*, Vol. **II**: *Radar Remote Sensing and Surface Scattering and Emission Theory*, Addison-Wesley, Reading, MA.

Wait, J.R. (1986) *Introduction to Antennas and Propagation*, Peter Peregrinus, London.

Wu, S.T. and Fung, A.K. (1972) A non-coherent model for microwave emission and backscattering from the sea surface. *Journal of Geophysical Research*, **77** (30), 5917–5929.

Xu, F. and Jin, Y.Q. (2006) Imaging simulation of polarimetric synthetic aperture radar remote sensing for comprehensive terrain scene using the mapping and projection algorithm. *IEEE Transactions on Geoscience and Remote Sensing*, **44** (11), 3219–3234.